Enhanced tameness by *Limosilactobacillus reuteri* from gut microbiota of selectively bred mice

Bhim B. Biswa[1,2], Hiroshi Mori[2,3], Atsushi Toyoda[4], Ken Kurokawa[2,5], Tsuyoshi Koide[1,2] *

[1]Mouse Genomics Resource Laboratory, National Institute of Genetics, Mishima, Shizuoka, Japan

[2]Graduate Institute for Advanced Studies, SOKENDAI, Mishima, Shizuoka, Japan

[3]Genome Diversity Laboratory, National Institute of Genetics, Mishima, Shizuoka, Japan

[4]Comparative Genomics Laboratory, National Institute of Genetics, Mishima, Shizuoka, Japan

[5]Genome Evolution Laboratory, National Institute of Genetics, Mishima, Shizuoka, Japan

*Correspondence should be addressed to TK. Email: tkoide@nig.ac.jp

Abstract: Domestication alters animal behaviour, primarily their tameness. We examine the effect of gut bacteria on tameness in mice. We examined gut microbiota in mice bred for active tameness by analysing faecal samples from 80 mice through shotgun metagenomic analysis. Selection for tameness did not substantially alter the gut microbiota's taxonomic or functional diversity. However, we observed an increased abundance of *Limosilactobacillus reuteri* in the selected groups and higher pyruvate levels in their plasma. We isolated *L. reuteri* strains secreting extracellular pyruvate, and administrated the cultured bacteria through drinking water. Mice treated with *L. reuteri* showed abundance of bacteria in the gut and a high level of active tameness compared to the control. This study elucidates the potential role of *L. reuteri* in the domestication process.

Introduction:

Domestication is a sustained multigenerational process by which captive animals adapt to humans and their environment. Several factors have been proposed to contribute to the adaptation of animals to captive environments. Most adaptation processes are explained by genetic changes; however, other factors such as certain experiences and environments, proximity and handling by humans(*1-3*), temperature(*4-6*), and food(*7*) may also contribute to the adaptation process. Therefore, domestication is a combination of genetic changes that occur over generations and of environmentally induced ontogenic events(*8*). Multiple studies have shown that gut microbiota influence host behaviour, brain development, and cognition. The metabolites produced by the microbiota alter the host's metabolic pathways or influence their immune system(*9, 10*). Several studies have explored the association between gut microbiota and domestication in animals, such as mice(*11*), horses(*12, 13*), buffalo(*14*), turkeys(*15*), chicken(*16*), and several animal species together(*17*). These studies have identified multiple species of bacteria that may influence the process of animal domestication. However, such studies are limited by the risk of contamination of the gut microbiota due to a non-sterile housing environment, the lack of common ancestors of test and control animals, differences in feed and water between test animals, crossover contamination from other animal species, and the use of antibiotics during rearing.

These challenges can be mitigated by using animals bred in a controlled setting with a singular focus on phenotypic selection and well-documented lineages. The WHS mice, which have been selectively bred for tameness are a good example of this approach. Tameness is a behavioural phenotype necessary for animals to adapt to humans and presents in two types: the motivation to approach humans (active tameness) and a reluctance to avoid humans (passive tameness). To increase active tameness, mice that exhibited a relatively high motivation to approach humans in the active tameness test, which evaluates levels of active tameness in mice(*18*), were bred selectively using wild-derived heterogeneous stock (WHS) mice. A founder group of WHS mice was developed by crossing eight different wild inbred strains originating from different countries and from three subspecies groups of *Mus musculus domesticus, castaneus and musculus(19, 20).* A group of WHS was bred with 16 pairs of mice in each generation to maintain high genetic diversity. Four groups of WHS were generated from the common founder WHS group by splitting them into two selected (S1 and S2) and two non-selected WHS groups (C1 and C2) (Figure 1A). Possible genetic components of active tameness

have been reported in these WHS mice(*20, 21*), suggesting that genetic factors play a major role in the control of tameness; however, the role of the gut microbiota still needs to be investigated. All WHS mice were kept in the same animal room but groups were kept isolated in different breeding racks. Furthermore, all the mice including the founder wild inbred strains were kept in specific pathogen-free (SPF) conditions and were given radiation-sterilised food and ultrafiltration-sterilised water. Therefore, any gut microbiota difference between selected and non-selected groups can be directly associated with the selective pressure on the host.

In our study, to characterize the gut microbiota in WHS mice, we conducted metagenomic analysis using genomic DNAs obtained from the faeces of animals from the selected and non-selected groups. An intervention strategy was then used to introduce specific bacteria into the drinking water of the mice to examine changes in their tameness behaviour.

Results:

Selective breeding leads to increase in active tameness behaviour

At the 27th generation of breeding, we examined tameness-related behaviours in the selected and non-selected groups of mice. We conducted tests of active tameness, passive tameness, and stay-on-hand tests on 80 mice: 10 male and 10 female mice for each group (Figure 1B, C, D, E). As S1 and C2, and S2 and C1 are genetically closely related (Figure 1A), we compared the data between the two pairs to determine the effect of selective breeding on active tameness compared to the non-selected control, hereafter. Data on nine behavioural parameters (Table S1)—heading, contacting, locomotion, and jumping in the active tameness test (Figure 1F, G, H, I); heading, accepting, locomotion, and jumping in the passive tameness test (Figure 1J, K, L, M); and median staying time in the stay-on-hand test (Figure 1N)—were obtained. Given that there was no effect of sex in the two-way analysis of variance (Two-way ANOVA; Table S2), data from both sexes were combined in all tameness analyses. From the clustering analysis of all nine parameters, we identified two significant clusters that categorize the parameters as either positively or negatively associated with tameness (Figure S1). For active contacting, compared to their respective control, both S1 ($p < 0.001$) and S2 ($p < 0.001$) exhibited significantly longer contacting durations than their respective controls (Figure 1G). Other tameness-related parameters, such as heading in the active tameness test (Figure 1F) (S1, $p < 0.001$; S2, $p < 0.05$), heading (Figure 1H) (S1, $p < 0.001$; S2, $p < 0.001$) and accepting (Figure 1I) (S1, $p < 0.001$; S2, $p < 0.01$) in the passive tameness test were higher in the selected groups than in the non-selected

groups. In the stay-on-hand test, mice of the selected groups stayed on the hand longer than controls (S1, $p < 0.001$; S2, $p < 0.001$) (Figure 1J). In contrast, parameters that are characteristic of wild mice, such as active jumping (Figure 1L) (C2, $p < 0.001$), passive locomotion (Figure 1M) (C2, $p < 0.001$; C1, $p < 0.05$), and passive jumping (Figure 1N) (C2, $p < 0.001$; C1, $p < 0.01$), were higher in the non-selected groups than in the selected groups. Collectively, S1 and S2 showed higher active and passive tameness than the non-selected group.

Subsequently, we investigate whether the changes in tameness due to selective breeding have resulted in changes in gut bacteria, or whether gut bacteria are involved in tameness in some other way.

Gut microbiome repertoire in mice of selected and non-selected groups

To examine the gut microbiota of the selected and non-selected groups, shotgun metagenomic sequencing analysis was performed on 80 faecal samples collected from each mouse after the tameness test. On average, we obtained 31 million paired reads per sample. Metagenome-assembled genomes (MAGs) were used to analyse the gut microbiome composition of WHS mice. Because the gut microbiota is a complex flora, we employed two assemblers and multiple binning approaches to obtain MAGs and recover as many good-quality MAGs as possible (Figure S2A). Using these approaches, we generated 14,816 MAGs (details of MAGs obtained from each binner are shown Figure S2B, C). After removing the redundant MAGs, we obtained 374 bacterial MAGs that were more than 50% completeness and had less than 10% contamination (Figure 2, S2E, Table S3). Of these MAGs, 226 were high-quality as they were more than 90% completeness and less than 5% contamination (Figure S2D). These 374 MAGs spanned 11 phyla, with 281 MAGs belonging to the *Bacillota A* phylum (Figure 2, Table S3). Upon comparing with the comprehensive mouse microbiota genome catalogue(*22*), we identified 27 species level novel MAGs that have not been previously reported. This is further confirmed by “taxonomic check” in DFAST(*23*). Of these 27 MAGs, one each belonged to *Actinomycetota*, *Bacillota B*, and *Patescibacteria*, eight to *Bacillota*, and 16 to *Bacillota A* (Figure 2). Additionally, despite the efficacy of machine learning binners in deriving higher quantity and quality MAGs, their limitations in binning all bacteria types were identified, suggesting that the application of combined methodology that integrates both single assembly and co-assembly, as well as the application of multiple binning tools is advantageous (Figure S2E).

Selective breeding for active tameness did not affect taxonomic diversity of gut microbiota

For taxonomic analysis, to capture the full diversity of WHS mice gut microbiome, we used the full NCBI/RefSeq prokaryote genome sequence database (NCBI RefSeq Complete V205) (*24*). We identified 665 bacterial species spanning 11 phyla, 21 classes, 45 orders, 103 families, and 339 genera (Figure 3A). Of these, 427 species were common to all four groups and contributed 99.8% abundance in all samples (Figure 3B).

Taxonomic beta diversity, which was calculated using Bray-Curtis dissimilarity, was not different between the groups (Figure 3C). Regarding alpha diversity indexes, Chao1 was significantly higher in C1 than in S1 ($p < 0.001$) and C2 ($p < 0.05$). S2 also had a higher Chao1 richness than S1 ($p < 0.05$) (Figure 3D). The Shannon diversity index was similar in all groups (Figure 3E). Overall, we found that the host selection pressure for tameness behaviour did not have any consistent influence on the overall taxonomic diversity of the gut microbiota in mice. We also did not find any significant difference in functional diversity between non-selected and selected mice (supplementary text).

We conducted Pearson correlation analysis on the tameness parameters scores with 40 significant taxa identified from the random forest analysis. This analysis highlighted that several *Lactobacillus* bacteria showed a significant positive correlation with both active and passive jumping behaviours, while showing a significant negative correlation with active heading. On the other hand, *Bacteroides sp.* CBA7301, *Ligilactobacillus animalis*, and *Prevotella bivia* were significantly positively correlated with our selection pressure- active contacting (Figure 3F).

The selected groups exhibited abundance in *Limosilactobacillus reuteri*

To identify the enrichment of bacterial species in tame mice and make the association more robust, we compared each selected group with its respective control group. For this analysis, we used MaAsLin2 to associate species-level gut microbiome composition with the WHS mouse group (Figure 3G, H). For MaAsLin2 analysis, only species that were significantly associated in both groups were considered to differ in abundance. We found that *Limosilactobacillus reuteri* (Figure 3I, J), previously known as *Lactobacillus reuteri*, one of the lactic acid bacteria, and *Candidatus* Gallimonas intestinalis (Figure 3K, L) were enriched in both selected groups compared to their respective controls.

Among the 374 MAGs generated, one high-quality MAG from *L. reuteri* and six MAGs of *Candidatus* Gallimonas genus were obtained. To quantify gut bacterial abundance, we used

CoverM for mapping reads to all MAGs, with mapping rates ranging from 75% to 93% (Figure S3A). Similar to Figure 3 (the Kraken2 results), we found that *L. reuteri* was significantly enriched in both selected groups compared to non-selected groups (S1, $p < 0.05$; S2, $p < 0.001$) (Figure S3 B, C). However, the relative abundance of the six *Candidatus* Gallimonas MAGs did not show a significant difference between the selected and non-selected groups (Figure S3D-I). These results combined with those of the Pearson correlation analysis performed earlier (Figure 3F) indicate that *L. reuteri* is the only bacterium that is consistently associated with tameness across our analyses. This association suggests that *L. reuteri* is linked with increased active tameness in the selected groups.

The selected groups have a higher level of plasma pyruvate

The influence of the gut microbiota on animals occurs through the production of metabolites that are absorbed into the host and change its behaviour. To identify the metabolites that may contribute to changes in tameness, we conducted a metabolomic analysis of plasma samples obtained from WHS mice. From the capillary electrophoresis time-of-flight mass spectrometry (CE-TOFMS) measurements, 281 peaks (179 in cation mode and 102 in Anion Mode) were detected and annotated according to HMT's standard library and the known-unknown peak library. Among the target metabolites, 70 (46 in cation mode and 24 in Anion Mode) were detected and quantified (Table S5). Correlation clustering of 70 metabolites did not show any visible difference between the control and selected groups (Figure 4A). Of these, four metabolites were significantly higher in selected mice (Figure 4B-E). To strengthen our findings, we performed MaAsLin2 analysis and after FDR correction, only pyruvic acid remained significantly associated with selected mice (Table S5). Plasma lactic acid concentration was also observed as it remains in homeostasis with pyruvic acid inside the body (Figure 4F).

***L. reuteri* administration increase tameness behaviour in non-selected mice**

To confirm the effects of *L. reuteri* and pyruvate in mice, strains that secrete more and less pyruvate were isolated and administered through drinking water. We isolated the bacterium from cecum material and faeces of the selected group of WHS mice. We isolated 22 *L. reuteri* strains using a specialized media with raffinose and found that 6 colonies secreted pyruvate into GAM culture media via biochemical assays (Figure 5A). *Lactobacillus helveticus* JCM1120, which is known as a pyruvate-secreting bacterial species (*25*), was used as a positive control of pyruvate secreting strain. Additionally, we assessed D-lactate and L-lactate secretion due to their homeostatic relationship with pyruvate (Figure 5A). In the experiment of bacterial strain

administration to C1 group mice, we chose NIG-A41 (high-pyruvate secreting strain), NIG-23 (low-pyruvate-secreting strain), as well as the *L. helveticus* JCM1120. After administration of the cultured bacterial strains for 21 days through drinking water to non-selected C1, tameness tests were conducted (Figure 5B). Mice treated with pyruvate secreting *L. reuteri*, NIG-A41, showed significantly increased active tameness compared to the PBS-administered group ($p < 0.05$) and *L. helveticus* administered group ($p<0.05$) (Figure 5C). Despite being insignificant, mice treated with less pyruvate secreting strain, NIG-23, showed higher active tameness than the PBS-treated mice. However, mice treated with *L. helveticus* did not show elevation in the active tameness compared with the PBS-treated mice. Active heading was also higher in NIG-A41 treated group but the difference was not significant (Figure 5D). Stay-on-hand test, passive heading, and passive accepting did not show prominent increase in NIG-A41 treated group (Figure 5E-G). Serum pyruvate level was higher in *L. helveticus* treated group ($p<0.05$) but neither NIG-A41 nor NIG-23 treated mice showed any difference in serum pyruvate levels compared to the PBS treated group (Figure 5H). We also examined the colonization of these bacterial strains in host mice by quantitative PCR analysis of the bacterial DNA obtained from faeces. Significantly higher levels, more than 1500 times in average, of the *L. reuteri* genomes were found in the faeces of both NIG-A41 ($p<0.01$) and NIG-23 ($p<0.001$) treated mice compared with the PBS-treated mice (Figure 5I). In contrast, the mice treated with *L. helveticus* JCM1120, which was originally isolated from Emmental (Swiss) cheese(*26*), did not show significant increase in the mice faeces (Figure 5J). We also monitored body weight changes and water intake during the administration period, but no significant differences among the groups were observed (Figure S4 A-D).

Discussion

In this study, we investigated the relationship between gut microbiota and active tameness behaviour and investigated its potential underlying mechanisms. We studied the gut microbiota in selected groups of mice that exhibited high tameness and in the non-selected groups of mice that exhibited low tameness. Our findings reveal that while selection for tameness does not markedly change the taxonomic or functional diversity of the gut microbiota, and leads to the enrichment of one specific bacterial species, *L. reuteri*, in tame mice. Furthermore, our plasma metabolic analysis revealed a significant elevation of pyruvate levels in tame mice. The

administration of pyruvate-secreting *L. reuteri* leads to elevation in the active tameness behaviour in non-selected mice.

The gut microbiota can alter host energy and lipid metabolism by producing energy metabolites, such as pyruvate, fumaric acid, and citric acid, and by influencing triglyceride levels in the host plasma(*27*). Pyruvate originating from the gut microbiome is absorbed by the host and contributes to the priming of the immune system and protection against *Salmonella* infection. This pyruvate is secreted by *L. helveticus*(*25*), a species that is very similar to *L. reuteri*. High circulating pyruvate levels in the blood and brain may also protect against Alzheimer's disease(*28*) by reducing age-related cognitive decline(*29*). In the present study, we found that mice with high active tameness had high plasma pyruvate levels (Figure 4A).

Twenty-two strains of *L. reuteri* were isolated by culturing colonies on selective media, six of which showed pyruvate secretion into GAM medium, which is a novel finding(*25*). The results provide important information for understanding how pyruvate secreted by *L. reuteri* affects brain function. Previous studies have linked *L. reuteri* administration to altered social behaviours in mice(*30-32*). Our study showed that *L. reuteri* increased active tameness, although pyruvate was not interpreted as a direct cause. We also found that bacteria isolated from the same host species exhibited more optimized colonization, without the sex-based colonization differences reported by Donovan et al. (*32*). Administration of *L. reuteri* through drinking water surged the populations over 1500-fold (Figure 5I), and this large change of *L. reuteri* levels likely contributed to the observed increase in tameness.

Our results underscore the host genetics' pivotal role in tameness, with C1 mice showing a less pronounced tameness level after *L. reuteri* administration (Figure 5C) compared to S1 and S2 groups (Figure 1G). This indicates that while the gut microbiota may influence behaviour, changes in host genetic factors are a major factor in changes in tameness during the selective breeding. Despite these facts, the result that long-term administration of live *L. reuteri* via drinking water can significantly increase the behaviour of tameness by vastly increasing its population in the gut is noteworthy for future studies.

The role of *L. reuteri* in influencing tameness behaviour warrants further investigation to elucidate the underlying mechanisms. Previous research by Matsumoto et al.(*21*) indicated that in WHS mice selected for tameness, there is a higher expression of oxytocin receptor in the hippocampus. In addition, tameness selection was found to lead to increases in sociability in WHS mice(*33*). Complementarily Poutahidis et al.(*34*) observed that administration of *L. reuteri*

through drinking water increased plasma oxytocin levels in C57BL/6 mice. This administration was also associated with an increase in oxytocin-positive neurons in the paraventricular nucleus (PVN) of the hypothalamus(*30, 31*). Sgritta et al.(*35*) demonstrated that *L. reuteri* communicates with the brain, thereby affecting social behaviour via the vagus nerve. Buffington et al.(*36*) identified that the gut microbiota metabolite tetrahydrobiopterin, enhanced by *L. reuteri*, can alleviate social deficits in germ-free mice, a process linked to increased oxytocin release(*37*). Danhof et al. (*38*) discovered that oxytocin is produced and secreted by intestinal epithelium enterocytes, triggered by *L. reuteri*. These collective findings pave the way for a hypothesis that oxytocin might be a central player in how *L. reuteri* influences tameness behaviour.

Overall, our findings contribute to the growing body of knowledge about the complex relationships between behaviour, the host genome, and the gut microbiota in the context of animal domestication. The potential link between *L. reuteri* and oxytocin pathways opens new avenues for exploring the biological basis of domestication and tameness in animals.

Materials and Methods

Experimental Conditions

All experiments in this study were conducted in strict accordance with the guidelines and protocols sanctioned by the Committee for Animal Care and Use at the National Institute of Genetics (permit number: R4-25). The mice used in our experiments were bred and maintained in specific pathogen-free (SPF) conditions within the animal facility at NIG. All equipment used for animal maintenance, including standard-sized transparent polycarbonate cages, cage tops, paper bedding materials, and other essential supplies, underwent sterilization through autoclaving. The mice were provided with a standard chow diet, CE-2 (CLEA Japan, Inc., Tokyo, Japan), which was radiation-sterilized at 15 KGy. Both food and ultrafiltration sterilized water (supplemented with 3 ppm chlorine) were availed to the mice ad libitum. The mice were housed in a temperature-controlled room at 23 ± 2°C with a humidity range of 50 ± 10% and a 12-h light-dark cycle with lights switched on at 6:00 am. Mice were weaned at approximately 3–4 weeks of age and were co-housed with their same-sex littermates until the tameness test was conducted. During cage changes and behavioural tests, each mouse was gently handled by its tail using tweezers covered with a silicone tube to minimize stress. All personnel involved in the experiments wore polyester suits, non-woven fabric masks, and double gloves (cloth gloves under latex gloves) to maintain a sterile environment. In all experiments, we took careful

measures to prevent microbiome cross-contamination. Cages housing mice from different groups were not placed in close proximity to each other. This precaution ensured that the microbial environments of each group remained distinct and uncontaminated by other groups. The first set of experiments was carried out using mice from the 27th generation of the WHS.

Selective breeding of WHS

WHS mice were generated by crossing eight wild strains, BFM/2Ms, PGN2/Ms, HMI/Ms, NJL/Ms, BLG2/Ms, KJR/Ms, CHD/Ms, and MSM/Ms, derived from different countries to expand the genetic heterogeneity. The founder stock, which is kept with 16 pairs of breeding, was split into two groups in the third generation to create S1 and C1, and, henceforth, S1 was selectively bred for higher active tameness. In the fifth generation, another selected group, S2, was split from C1, and another non-selected group, C2, was split from S1. Thereafter, S2 was selectively bred for a higher level of active tameness and C2 was maintained as the non-selected group. Mice used for mating were selected from each of the five females and five males offspring of each pair based on the highest contacting score in the active tameness test, and if two or more animals showed the same highest contacting score, the individual with the higher heading score in the same test was selected.

Tameness test

The tameness test was performed at six weeks of age, as described in a previous study(*18*) during the light period between 14:00-17:00. The test was conducted in an open-field arena (40 × 40 × 40 cm) made of grey polyvinyl chloride (O'Hara & Co. Ltd., Tokyo, Japan) with the floor illuminated with approximately 100 lux at the centre (*39, 40*). The tameness test was a three-min protocol divided into one minute each of the active and passive tameness tests and three trials of the stay-on-hand test. In the active tameness test, the experimenter's hand was kept 10 cm away from the test mouse for 1 min with the fingers moving slightly and rhythmically to observe the animal's motivation to approach and contact the human hand. In the passive tameness test, the experimenter attempted to touch the mouse with their hand, and mouse behaviour was recorded for 1 min. This test examined how long the mice could tolerate being touched by a human hand. In the stay-on-hand test, each mouse was picked from its tail using silicon-coated tweezers, placed on the experimenter's hand, and stroked gently until it attempted to get off the hand. All tests were video-recorded and analysed by another experienced researcher, M. Nihei, using TanaMove (http://www.mgrl-lab.jp/MGRL_software.html) and scores were assigned to nine

different parameters. The detailed step-by-step process has been outlined in previous studies(*39, 40*).

Tameness test parameter clustering

The analysis was performed in R version 4.3.2. The tameness test results for all 80 samples were normalized using "min-max" normalization. Clustering was executed based on the correlation distance, employing the Ward method via the "hclust" function. The statistical significance of the identified clusters was assessed using the "pvclust" function from the R package pvclust (version 2.2.0)(*41*), setting the significance level at 5% for each clustering analysis.

Mice faeces collection

In all experiments, mouse faecal samples were collected following the tameness test, ensuring consistency in timing between 17:00 and 18:00 on the same day. To maintain sterility and minimize environmental variables, the test mice were housed in autoclaved, sterile cages devoid of any bedding material. This setup allowed for natural defecation without external prompting. The faeces were carefully collected in an Eppendorf tube using sterile aluminium foil and immediately stored at -80˚C.

Blood serum and plasma collection

Blood plasma was obtained when mice reached 11 weeks of age. For the collection procedure, the mice were first anaesthetized using an intraperitoneal (IP) injection of pentobarbital at a dosage of 50 mg/kg body weight (Sigma-Aldrich, USA). Following anaesthesia, blood samples were drawn via cardiac puncture using a syringe pre-treated with heparin to prevent coagulation. The collected blood was then transferred into heparinized Eppendorf tubes. These tubes were allowed to stand undisturbed at room temperature for 30 min to enable the separation of blood components. Subsequently, the tubes were centrifuged at 10,000 G for 10 min at a temperature of 4°C. For serum isolation, the same protocol was used, excluding heparin treatment.

Metagenomic DNA isolation from mice faeces

In our modified approach to metagenomic DNA isolation, we utilized protocol #6 from Costea et al.(*42*), incorporating the QIAamp Fast DNA Stool Mini Kit (QIAGEN GmbH, Hilden, Germany) for DNA extraction. The process began with treating 180–220 mg of faecal samples with 1 ml of lysis buffer (500 mM NaCl, 50 mM Tris-HCl at pH 8.0, 50 mM EDTA, and 4% sodium dodecyl sulfate). This mixture was homogenized for 5 min using a handheld homogenizer (Leda Trading Corp.), followed by the addition of 10 µl proteinase K and sterile zirconia beads (1.0 mm, 20-30; BioSpec, Inc., USA). For thorough mixing, the sample was

vortexed at maximum speed for 10 min using a Vortex-Genie 2 mixer (MO BIO Laboratories, Inc., USA) and then incubated at 95°C for 15 min. Post incubation, the sample was centrifuged at 16,000 x g for 5 min at 4°C, and the supernatant was transferred to a new 2 mL tube. The remaining pellet was subjected to a second round of lysis, resuspended in 300 µL of the lysis buffer, and processed as previously described. The combined supernatants from both lysis steps were then treated with 260 µL of 10 M ammonium acetate, followed by vortexing and incubation on ice for 5 min. The solution was centrifuged at 16,000 x g for 10 min at 4°C, and the resulting supernatant was equally divided into two 1.5 mL tubes, each containing 750 µL isopropanol. These tubes were then incubated on ice for 30 min and centrifuged at 16,000 x g for 15 min. The supernatant was discarded, and the pellet was washed with 0.5 mL of 70% ethanol and left to air-dry. Finally, the dried pellets were reconstituted in 100 µL of TE (Tris-EDTA) buffer, and the aliquots were pooled. We added 2 µL DNase-free RNase (10 mg/mL) to the pooled DNA solution and incubated it at 37°C for 15 min. Then, 10 µL proteinase K and 200 µL buffer AL were added, vortexed for 15 s, and incubated at 70°C for 10 min. Subsequently, 200 µL of 96–100% ethanol was added to the lysate, vortexed, and passed through a QIAamp spin column, and centrifuged for 1 min. The filtrate was discarded and the column was sequentially washed with 500 µL each of Buffer AW1 and AW2. Following a final centrifugation, 100 µL AE Buffer was used to elute DNA into a new 1.5 mL tube. A spectrophotometer (NanoVue Plus) was used for the quality check. A Qubit 2.0 Fluorometer was used for precise quantification following the manufacturer's instructions. DNA integrity was checked using 0.8% agarose gel electrophoresis. The DNA was then stored at -20°C for future use.

Shotgun metagenomic sequencing

Library preparation and sequencing were performed at the Advanced Genomics Center of the National Institute of Genetics**.** Briefly**,** genomic DNA was fragmented to an average size of 500 bp using a DNA shearing system (M220 focused ultrasonicator; Covaris Inc., MA. USA). A paired-end library was constructed using a TruSeq DNA PCR-Free Library Prep kit (Illumina, CA, USA) and size-selected on an agarose gel using a Zymoclean Large Fragment DNA Recovery Kit (Zymo Research, CA. USA). The final library was subjected to paired-end sequencing using an Illumina NovaSeq 6000 sequencer with a read length of 150 bp.

Plasma metabolites analysis

For metabolomic analysis, samples were analysed by Human Metabolome Technologies, Inc. (https://humanmetabolome.com/jpn/). A basic scan was performed to detect more than 1000

water-soluble metabolites. The protocol for this analysis has been described previously(*43-46*). Briefly, metabolome analysis (CE-TOFMS) was performed on 12 randomly selected mouse plasma samples in two modes for cationic and anionic metabolites.

***Limosilactobacillus reuteri* isolation**

Cecum and faecal samples were collected from mice of selected group (S1), mixed, and then serially diluted. This diluted mixture was cultured on *L. reuteri* Isolation Media (LRIM)(*47*) agar plates, with raffinose (Tokyo Chemical Industry Co. Ltd, Japan) as the sole carbon source. The plates were incubated for 48 h at 45°C under anaerobic conditions (5% CO_2). To maintain the anaerobic condition, plates were stored in a sealed box containing one AnaeroPack sachet (Mitsubishi gas chemical company, Inc, Japan). For the isolation of pure cultures, selected colonies were first streak plated twice on LRIM plates. This was followed by third streak plating on De Man–Rogosa–Sharpe (MRS) (Sigma-Aldrich, USA) agar plate.

***Limosilactobacillus reuteri* phylogenetic analysis**

All isolated colonies were cultured in MRS media, after which DNA was extracted using the NucleoSpin Microbial DNA kit (Takara Bio Inc., Shiga, Japan), according to the manufacturer's protocol. To amplify the full 1.6 kbp region of the 16S rDNA, polymerase chain reaction (PCR) was performed using the universal primers bak4 (5'-AGGAGGTGATCCARCCGCA-3') and bak11w (5'-AGTTTGATCMTGGCTCAG-3')(*48, 49*). Cycling conditions were 95°C for 5□min, followed by 35□cycles of 95°C for 15□s, 60°C for 30□s and 72°C for 2 min, and final extension for 7 min at 72°C. The PCR cycling conditions included an initial denaturation at 95°C for 5 min, followed by 35 cycles of 95°C for 15 s, 60°C for 30 s, and 72°C for 2 min, with a final extension at 72°C for 7 min. The PCR products were then purified and subjected to Sanger sequencing. Taxonomic identification of obtained sequences was done using NCBI BLASTn(*50*). To infer phylogeny, along with our sequences, we first obtained 16S rRNA gene sequence of multiple *Limosilactobacillus* species from NCBI along *Lactobacillus helveticus* as outgroup. All sequences were aligned using the MAFFT online server with "FFT-NS-I" command (*51, 52*). Using Model finder (*53*), we found "TPM3u+F+I" as the best-fit model for out data. We used IQ-TREE 2 (*54*) with 1000 bootstrap to construct a maximum likelihood tree. This tree was edited using iTOL online server (*55*).

Pyruvate, L-Lactate, and D-Lactate secretion assay

In this experiment, *L. helveticus* (JCM1120), sourced from the Japan Collection of Microorganisms (JCM), served as the positive control for pyruvate production. All bacterial

strains, including the control, were cultured in Gifu Anaerobic Broth (GAM) medium (Nissui Pharmaceutical, Japan), which was supplemented with 1% glucose. The incubation was conducted for 24 h at 37°C under anaerobic conditions. To measure the concentrations of pyruvate, L-Lactate, and D-Lactate in the media, we utilized biochemical assay kits from Cayman Chemicals (Michigan, USA), strictly adhering to the manufacturer's protocol.

***Limosilactobacillus reuteri* administration**

All bacterial strains were cultured in MRS media for 24 h. Following this cultivation, the optical density (OD) at 600 nm was measured to estimate the number of bacteria in the solution, using a standard curve. The bacteria were then washed with PBS, resuspended in PBS, and stored at -80˚C until use. We cultured a fresh batch of bacteria every week to maintain viability. PBS (vehicle) or bacteria (~1 × 10^8 CFU/Cage/day) was added to the drinking water of the mice each day between 17:00 and 18:00. Mice from the 37th generation of C1 group were used. For the drinking water administration and measurements, 15-mL glass test tubes stoppered with silicone caps with double ball-bearing nozzles, Drinko-measurer DM-G1 (O'hara & Co. Ltd., Tokyo, Japan), were used daily. The administration of *L. reuteri* began immediately post-weaning, at approximately 3 weeks of age, and was continued for 21 days. To minimize isolation stress, mice were housed in same-sex pairs. Faecal samples were collected from each individual both before the start and at the end of the experimental period. In addition, we monitored and recorded the daily water consumption of each cage and measured the body weight of the mice at the end of the experiment. After the 21-day bacterial administration period, a tameness test was conducted. This was followed by the collection of faecal and plasma samples for further analysis.

qPCR quantification of Limosilactobacillus reuteri and Lactobacillus helviticus

Quantitative PCR (qPCR) was conducted using a Thermal Cycler Dice Real Time System III (Takara Bio Inc., Shiga, Japan). For each 25 μL reaction, TB Green Premix Ex Taq II (Tli RNaseH Plus) (Takara Bio Inc., Shiga, Japan) and gene-specific primers at a concentration of 1 μM were used. The reaction mixtures included 5 ng of metagenomic DNA, the quantity of which was determined using Qubit. The cycling conditions were set at 95°C for 5 min, followed by 40 cycles of denaturation at 95°C for 20 s, annealing at 62°C for 20 s, and extension at 72°C for 30 s. After the PCR cycles, a melt curve analysis was performed in the range of 60–95°C using the default settings of the system. The primers used in the qPCR were as follows: Universal

bacterial primers EUB338 (*56*) (5'-ACTCCTACGGGAGGCAGCAG-3'), and EUB518 (5'-ATTACCGCGGCTGCTGG-3')(*57*); *L. reuteri* -specific 16S-23S rRNA gene spacer primers, sg-Lreu-F (5'-GAAGATCAGTCGCAYTGGCCCAA-3'), and sg-Lreu-R (5'-TCCATTGTGGCCGATCAG-3')(*58*); *L. helveticus* hsp60 specific primers, F1LHelHsp (5'-CTTTGATCGCTGATGCTATGGAAAAGGTTGGTC-3'), and R1LHelHsp (5'-GATCAACAATGACTTGCCTTGTTGAACAATTTC-3')(*59*). The qPCR analysis was based on the ΔCt of the specific primers normalized to the ΔCt of the universal primers (ΔΔCt method).

Bioinformatics analysis of metagenomic sequence data

Quality control of metagenomic sequences

All sequencing reads obtained were quality-filtered using KneadData (Ver. 0.10.0), where low-quality sequences and any contamination from PhiX, host (mouse_C57BL_6NJ.1), human genome (hg37dec_v0.1.1), or transcriptome (human_hg38_refMrna.1) were discarded. KneadData uses Trimmomatic (Ver. 0.33)(*60*) to remove adapters, TRF(*61*) to remove repetitive sequences, and Bowtie2 (Ver. 2.4.5)(*62*) to remove contaminants.

Taxonomic analysis

Taxonomic analysis of the gut microbiome was conducted using Kraken 2 (Ver. 2.1.2)(*63*). We employed the full NCBI/RefSeq database made by Wright et al. (NCBI RefSeq Complete V205 (1189□GB))(*24*) to ensure comprehensive species identification within the gut samples. Default parameters were used for Kraken 2, with a confidence score threshold set at 0.15. This threshold was chosen to strike a balance between the robustness of species identification and maximizing the percentage of sequences utilized in the analysis. Further refinement of the Kraken 2 output was achieved through Bayesian re-estimation using Braken2 (Ver. 2.6.2), also utilizing its default settings(*64*).

Functional Analysis

For functional analysis in our study, we utilized HUMAnN3 (Ver. 3.0.1)(*65*) employing the '–bypass-prescreen' option. We concatenated the filtered forward and reverse sequences from each sample and mapped them to the comprehensive ChocoPhlAn database (Ver. 201901b). Sequences that remained unassigned after this step were further analysed against the UniRef90 database. To identify specific metabolic pathways, we employed the MetaCyc database(*66*). We obtained Copies per Million (CPM) data for each gene family and pathway using the 'humann_renorm_table' command.

Abundance and Diversity Analysis

Diversity analysis and graph generation in our study were carried out using the MicroEco R package(*67*) We normalized the abundance data obtained from Braken2 by rarefying it to the size of the smallest sample(*68*). To assess the statistical significance of alpha diversity, we employed the Kruskal–Wallis Rank Sum test. Beta diversity was analysed based on Bray-Curtis dissimilarity; analysis was complemented by principal coordinate analysis (PCoA), which was applied to both taxonomic and functional data. In our correlation analysis, we first conducted a random forest classification using 'randomForest' R package (*69*), utilizing mouse group information (C1, C2, S1, and S2) on the normalized Bracken2 bacterial abundance data, adjusting the p-value using the Benjamini-Hochberg False Discovery Rate (FDR) method. Afterward, we normalized the scores of tameness parameters through min-max normalization. This normalized tameness scores were then subjected to Pearson correlation with the top 40 significant taxa identified in the random forest analysis using 'pheatmap' R package (*70*) .

MaAsLin2 association analysis

For association between taxonomic abundance with each mice group, we use Bracken2 (Table S2) abundance data. Initially it was normalized using 'Total sum scaling', then transformed into a log scale, after which association analysis was performed. In association analysis between functional pathways, we did not perform additional normalisation or transformation as HUMAnN3's output was already normalized. In both analyses, we used a linear model and compared S1 and S2 groups to their respective controls.

MAG generation

Default settings were used in different software, unless otherwise specified. Filtered sequences were assembled using metaSPAdes (k =21, 33, 55) (Ver. 3.15.4)(*71*) for a single assembly or MEGAHIT (--k-min 21 --k-max 77) (Ver. 1.2.9)(*72*) for co-assembly. Multiple binners with different binning strategies were used. The MEGAHIT assembly was binned using MetaCoAG (Ver. 1.0)(*73*), MaxBin2 (Ver. 2.2.7)(*74*), and MetaBAT2 (Ver. 2.15)(*75*). This was followed by the generation of a nonredundant set of bins using DAStool (search_engine diamond) (Ver. 1.1.4)(*76*). For the metaSPAdes-generated assembly, we utilized SemiBin (multi_easy_bin) (Ver. 0.7.0) (*77*) and VAMB (multisplit) (Ver. 3.0.8)(*78*). All bins produced were subjected to contamination filtering using MDMcleaner (Ver. 0.8.3)(*79*). Bins devoid of chimeric sequences, as confirmed by GUNC (Ver. 1.0.5)(*80*), and those with MAG quality scores above 0.5 were retained for further analysis. These filtered bins were then evaluated for contamination and

completeness using CheckM (lineage_wf) (Ver. 1.2.0) (*81*). To create a nonredundant bin set, we employed the "dereplicate" command of dRep (Ver. 3.0.0) (-comp 50, -con 10, -pa 0.90, -sa 0.95, -nc 0.30, and -cm larger)(*82*). Finally, the taxonomic classification of all bacteria and the generation of the species tree were performed using GTDB-Tk (classify_wf) (Ver. 2.1.1) with the "r207_v2" database (*83*). MAGs phylogenetic tree was generated using FastTree (Ver. 2.1.11)(*84*) within GTDB-Tk using the "infer" command. The generated tree was then refined and edited using the Interactive Tree of Life (iTOL) tool (*55*).

MAG analysis

To identify novel MAGs, we utilized the 'compare' command of dRep (Ver. 3.0.0) (-pa 0.90 -sa 0.95 -nc 0.30 -cm larger) (*82*). This analysis was conducted on a combined database that included the 1573 mouse gut MAGs previously compiled by Kieser et al. (*22*) along with the 374 MAGs generated in our study. We classified our MAGs as novel if they did not cluster with any of the existing MAGs in this integrated database at 95% ANI, thereby distinguishing them as unique at species level. To quantify the relative abundance of each MAG, we employed CoverM (Ver. 0.6.1) (https://github.com/wwood/CoverM) and used minimap (*85*) to map reads to our MAG database. All 27 novel MAGs were annotated using DFAST (81) and submitted to DDBJ.

Statistical analysis

GraphPad Prism (version 10.1.2) was used for all statistical analyses. To evaluate the normality of the dataset, the Shapiro–Wilk test was utilized. For data that followed a normal distribution, one-way ANOVA was applied, with subsequent Tukey's test for multiple comparisons. In cases where data did not conform to normal distribution, the Kruskal–Wallis test was employed, followed by Dunn's test for multiple comparisons. To check the effect of sex on tameness behaviour, a two-way ANOVA was performed followed by Tukey's test for multiple comparisons. For statistical association analysis of plasma metabolites, taxonomic abundance, and functional abundance, MaAsLin2 (1.12.0)(*86*) was used with a Benjamini-Hochberg q-value of 0.25 following previous microbiome studies(*87, 88*). For MAGs abundance, two tailed Mann–Whitney U test was performed. For daily water intake, a two-way ANOVA was performed followed by Tukey's test for multiple comparisons. For mice body weight, the Kruskal–Wallis test was employed, followed by Dunn's test for multiple comparisons.

Acknowledgments: We appreciate Motoko Nihei, Akiko Tsuchiya, and Kyouhei Kurosawa for their technical assistance. Computations were partially performed on the NIG supercomputer at ROIS National Institute of Genetics.

Funding:

JST SPRING Grant Number JPMJSP2104 (BBB)

Grant-in-Aid for Scientific Research, JSPS KAKENHI Grant Number 19KK0177 (TK)

Research Organization of Information and Systems (ROIS) grant (TK)

Author contributions: B. B. B. and T. K. conceived the project and designed the experiments; B. B. B. performed the experiments and analysed the data; A. T. performed shotgun sequencing; H. M. and K. K. provided intellectual insights and guidance. T. K. provided supervision and funding; The initial draft of the manuscript was authored by B.B.B. and T. K., with the final Ver. being written collaboratively, incorporating feedback from all authors. Each author has approved the final version of the manuscript.

Competing interests: T.K. and B.B.B. applied for a patent (US 63/468017) regarding the findings of this study. The other authors declare no competing interests.

Data and materials availability: All data required to evaluate the conclusions of this study are presented in the paper or Supplementary Materials. The raw sequencing datasets generated in this study are available in the DDBJ Sequenced Read Archive under accession number DRA016414 (DRR480456-DRR480535). All 16S rDNA generated in this study can be accessed using following accession IDs (LC801559-LC801580). Non-redundant set of MAGs were submitted to zenodo database (10.5281/zenodo.8289507). No new code was generated in this study. The mouse stocks used in this study, S1, S2, C1, and C2, are available upon request from the following website https://grc.nig.ac.jp/mgrlab/index.xhtml .

Lead contact: Further information and requests for resources and reagents should be directed to the lead contact, Tsuyoshi Koide (tkoide@nig.ac.jp).

References

1. E. O. Price, Behavioral development in animals undergoing domestication. *Applied Animal Behaviour Science* **65**, 245-271 (2002).
2. A. Ebinghaus, S. Ivemeyer, U. Knierim, Human and farm influences on dairy cows responsiveness towards humans - a cross-sectional study. *PLoS One* **13**, e0209817 (2018).

3. S. E. Harris, J. Munshi-South, C. Obergfell, R. O'Neill, Signatures of rapid evolution in urban and rural transcriptomes of white-footed mice (Peromyscus leucopus) in the New York metropolitan area. *PLoS One* **8**, e74938 (2013).
4. K. Ganeshan, A. Chawla, Warming the mouse to model human diseases. *Nat Rev Endocrinol* **13**, 458-465 (2017).
5. M. Czarnoleski, B. S. Cooper, J. Kierat, M. J. Angilletta, Jr., Flies developed small bodies and small cells in warm and in thermally fluctuating environments. *J Exp Biol* **216**, 2896-2901 (2013).
6. S. E. Diamond, L. Chick, A. Perez, S. A. Strickler, M. R. A., Rapid evolution of ant thermal tolerance across an urban-rural temperature cline. *Biological Journal of the Linnean Society* **112**, 248-257 (2017).
7. F. Luca, G. H. Perry, A. Di Rienzo, Evolutionary adaptations to dietary changes. *Annu Rev Nutr* **30**, 291-314 (2010).
8. E. O. Price, *Animal domestication and behavior* (CABI Publishing, 2002).
9. J. F. Cryan, K. J. O'Riordan, C. S. M. Cowan, K. V. Sandhu, T. F. S. Bastiaanssen, M. Boehme, M. G. Codagnone, S. Cussotto, C. Fulling, A. V. Golubeva, K. E. Guzzetta, M. Jaggar, C. M. Long-Smith, J. M. Lyte, J. A. Martin, A. Molinero-Perez, G. Moloney, E. Morelli, E. Morillas, R. O'Connor, J. S. Cruz-Pereira, V. L. Peterson, K. Rea, N. L. Ritz, E. Sherwin, S. Spichak, E. M. Teichman, M. van de Wouw, A. P. Ventura-Silva, S. E. Wallace-Fitzsimons, N. Hyland, G. Clarke, T. G. Dinan, The Microbiota-Gut-Brain Axis. *Physiol Rev* **99**, 1877-2013 (2019).
10. L. H. Morais, H. L. t. Schreiber, S. K. Mazmanian, The gut microbiota-brain axis in behaviour and brain disorders. *Nat Rev Microbiol* **19**, 241-255 (2021).
11. K. L. Bowerman, S. C. L. Knowles, J. E. Bradley, L. Baltrūnaitė, M. D. J. Lynch, K. M. Jones, P. Hugenholtz, Effects of laboratory domestication on the rodent gut microbiome. *ISME Communications* **1**, 49 (2021).
12. J. L. Metcalf, S. J. Song, J. T. Morton, S. Weiss, A. Seguin-Orlando, F. Joly, C. Feh, P. Taberlet, E. Coissac, A. Amir, E. Willerslev, R. Knight, V. McKenzie, L. Orlando, Evaluating the impact of domestication and captivity on the horse gut microbiome. *Sci Rep* **7**, 15497 (2017).
13. L. Ang, G. Vinderola, A. Endo, J. Kantanen, C. Jingfeng, A. Binetti, P. Burns, S. Qingmiao, D. Suying, Y. Zujiang, D. Rios-Covian, A. Mantziari, S. Beasley, C. Gomez-Gallego, M. Gueimonde, S. Salminen, Gut Microbiome Characteristics in feral and domesticated horses from different geographic locations. *Commun Biol* **5**, 172 (2022).
14. V. R. Prabhu, Wasimuddin, R. Kamalakkannan, M. S. Arjun, M. Nagarajan, Consequences of Domestication on Gut Microbiome: A Comparative Study Between Wild Gaur and Domestic Mithun. *Front Microbiol* **11**, 133 (2020).
15. J. Craft, H. Eddington, N. D. Christman, W. Pryor, J. M. Chaston, D. L. Erickson, E. Wilson, Increased Microbial Diversity and Decreased Prevalence of Common Pathogens in the Gut Microbiomes of Wild Turkeys Compared to Domestic Turkeys. *Appl Environ Microbiol* **88**, e0142321 (2022).
16. L. C. Puetz, T. O. Delmont, O. Aizpurua, C. Guo, G. Zhang, R. Katajamaa, P. Jensen, M. T. P. Gilbert, Gut Microbiota Linked with Reduced Fear of Humans in Red Junglefowl Has Implications for Early Domestication. *Advanced Genetics* **2**, 2100018 (2021).
17. A. T. Reese, K. S. Chadaideh, C. E. Diggins, L. D. Schell, M. Beckel, P. Callahan, R. Ryan, M. Emery Thompson, R. N. Carmody, Effects of domestication on the gut microbiota parallel those of human industrialization. *Elife* **10**, (2021).

18. T. Goto, A. Tanave, K. Moriwaki, T. Shiroishi, T. Koide, Selection for reluctance to avoid humans during the domestication of mice. *Genes Brain Behav* **12**, 760-770 (2013).
19. T. Koide, T. Goto, T. Takano-Shimizu, Genomic mixing to elucidate the genetic system of complex traits. *Exp Anim* **61**, 503-509 (2012).
20. Y. Matsumoto, T. Goto, J. Nishino, H. Nakaoka, A. Tanave, T. Takano-Shimizu, R. F. Mott, T. Koide, Selective breeding and selection mapping using a novel wild-derived heterogeneous stock of mice revealed two closely-linked loci for tameness. *Sci Rep* **7**, 4607 (2017).
21. Y. Matsumoto, H. Nagayama, H. Nakaoka, A. Toyoda, T. Goto, T. Koide, Combined change of behavioral traits for domestication and gene-networks in mice selectively bred for active tameness. *Genes Brain Behav* **20**, e12721 (2021).
22. S. Kieser, E. M. Zdobnov, M. Trajkovski, Comprehensive mouse microbiota genome catalog reveals major difference to its human counterpart. *PLoS Comput Biol* **18**, e1009947 (2022).
23. Y. Tanizawa, T. Fujisawa, Y. Nakamura, DFAST: a flexible prokaryotic genome annotation pipeline for faster genome publication. *Bioinformatics* **34**, 1037-1039 (2018).
24. R. J. Wright, A. M. Comeau, M. G. I. Langille, From defaults to databases: parameter and database choice dramatically impact the performance of metagenomic taxonomic classification tools. *Microb Genom* **9**, (2023).
25. N. Morita, E. Umemoto, S. Fujita, A. Hayashi, J. Kikuta, I. Kimura, T. Haneda, T. Imai, A. Inoue, H. Mimuro, Y. Maeda, H. Kayama, R. Okumura, J. Aoki, N. Okada, T. Kida, M. Ishii, R. Nabeshima, K. Takeda, GPR31-dependent dendrite protrusion of intestinal CX3CR1(+) cells by bacterial metabolites. *Nature* **566**, 110-114 (2019).
26. S. Orla-Jensen, *The lactic acid bacteria* (Andr. Fred. Host and Son, Copenhagen, 1919), vol. 3.
27. V. R. Velagapudi, R. Hezaveh, C. S. Reigstad, P. Gopalacharyulu, L. Yetukuri, S. Islam, J. Felin, R. Perkins, J. Boren, M. Oresic, F. Backhed, The gut microbiota modulates host energy and lipid metabolism in mice. *J Lipid Res* **51**, 1101-1112 (2010).
28. E. Isopi, A. Granzotto, C. Corona, M. Bomba, D. Ciavardelli, M. Curcio, L. M. Canzoniero, R. Navarra, R. Lattanzio, M. Piantelli, S. L. Sensi, Pyruvate prevents the development of age-dependent cognitive deficits in a mouse model of Alzheimer's disease without reducing amyloid and tau pathology. *Neurobiol Dis* **81**, 214-224 (2015).
29. H. Koivisto, H. Leinonen, M. Puurula, H. S. Hafez, G. A. Barrera, M. H. Stridh, H. S. Waagepetersen, M. Tiainen, P. Soininen, Y. Zilberter, H. Tanila, Chronic Pyruvate Supplementation Increases Exploratory Activity and Brain Energy Reserves in Young and Middle-Aged Mice. *Front Aging Neurosci* **8**, 41 (2016).
30. S. W. Dooling, M. Sgritta, I. C. Wang, A. Duque, M. Costa-Mattioli, The Effect of Limosilactobacillus reuteri on Social Behavior Is Independent of the Adaptive Immune System. *mSystems*, e0035822 (2022).
31. S. A. Buffington, G. V. Di Prisco, T. A. Auchtung, N. J. Ajami, J. F. Petrosino, M. Costa-Mattioli, Microbial Reconstitution Reverses Maternal Diet-Induced Social and Synaptic Deficits in Offspring. *Cell* **165**, 1762-1775 (2016).
32. M. Donovan, C. S. Mackey, M. D. J. Lynch, G. N. Platt, A. N. Brown, B. K. Washburn, D. J. Trickey, J. T. Curtis, Y. Liu, T. C. Charles, Z. Wang, K. M. Jones, Limosilactobacillus reuteri administration alters the gut-brain-behavior axis in a sex-dependent manner in socially monogamous prairie voles. *Front Microbiol* **14**, 1015666 (2023).

33. B. Venkatachalam, B. B. Biswa, H. Nagayama, T. Koide, Association of tameness and sociability but no sign of domestication syndrome in mice selectively bred for active tameness. *Genes Brain Behav* **23**, e12887 (2024).
34. T. Poutahidis, S. M. Kearney, T. Levkovich, P. Qi, B. J. Varian, J. R. Lakritz, Y. M. Ibrahim, A. Chatzigiagkos, E. J. Alm, S. E. Erdman, Microbial symbionts accelerate wound healing via the neuropeptide hormone oxytocin. *PLoS One* **8**, e78898 (2013).
35. M. Sgritta, S. W. Dooling, S. A. Buffington, E. N. Momin, M. B. Francis, R. A. Britton, M. Costa-Mattioli, Mechanisms Underlying Microbial-Mediated Changes in Social Behavior in Mouse Models of Autism Spectrum Disorder. *Neuron* **101**, 246-259 e246 (2019).
36. S. A. Buffington, S. W. Dooling, M. Sgritta, C. Noecker, O. D. Murillo, D. F. Felice, P. J. Turnbaugh, M. Costa-Mattioli, Dissecting the contribution of host genetics and the microbiome in complex behaviors. *Cell* **184**, 1740-1756 e1716 (2021).
37. J. Ciosek, J. W. Guzek, Neurohypophysial function and pteridines: effect of (6R)-5,6,7, 8-tetrahydro-alpha-biopterin on bioassayed hypothalamo-neurohypophysial vasopressin and oxytocin in the rat. *Folia Med Cracov* **33**, 25-35 (1992).
38. H. A. Danhof, J. Lee, A. Thapa, R. A. Britton, S. C. Di Rienzi, Microbial stimulation of oxytocin release from the intestinal epithelium via secretin signaling. *Gut Microbes* **15**, 2256043 (2023).
39. H. Nagayama, Y. Matsumoto, A. Tanave, M. Nihei, T. Goto, T. Koide, Measuring Active and Passive Tameness Separately in Mice. *J Vis Exp*, (2018).
40. B. B. Biswa, T. Koide, in *Behavioral Neurogenetics. Neuromethods*, D. Yamamoto, Ed. (Humana, New York, NY, 2022), vol. 181, pp. 107-122.
41. R. Suzuki, H. Shimodaira, Pvclust: an R package for assessing the uncertainty in hierarchical clustering. *Bioinformatics* **22**, 1540-1542 (2006).
42. P. I. Costea, G. Zeller, S. Sunagawa, E. Pelletier, A. Alberti, F. Levenez, M. Tramontano, M. Driessen, R. Hercog, F. E. Jung, J. R. Kultima, M. R. Hayward, L. P. Coelho, E. Allen-Vercoe, L. Bertrand, M. Blaut, J. R. M. Brown, T. Carton, S. Cools-Portier, M. Daigneault, M. Derrien, A. Druesne, W. M. de Vos, B. B. Finlay, H. J. Flint, F. Guarner, M. Hattori, H. Heilig, R. A. Luna, J. van Hylckama Vlieg, J. Junick, I. Klymiuk, P. Langella, E. Le Chatelier, V. Mai, C. Manichanh, J. C. Martin, C. Mery, H. Morita, P. W. O'Toole, C. Orvain, K. R. Patil, J. Penders, S. Persson, N. Pons, M. Popova, A. Salonen, D. Saulnier, K. P. Scott, B. Singh, K. Slezak, P. Veiga, J. Versalovic, L. Zhao, E. G. Zoetendal, S. D. Ehrlich, J. Dore, P. Bork, Towards standards for human fecal sample processing in metagenomic studies. *Nat Biotechnol* **35**, 1069-1076 (2017).
43. T. Soga, D. N. Heiger, Amino acid analysis by capillary electrophoresis electrospray ionization mass spectrometry. *Anal Chem* **72**, 1236-1241 (2000).
44. T. Soga, Y. Ueno, H. Naraoka, Y. Ohashi, M. Tomita, T. Nishioka, Simultaneous determination of anionic intermediates for Bacillus subtilis metabolic pathways by capillary electrophoresis electrospray ionization mass spectrometry. *Anal Chem* **74**, 2233-2239 (2002).
45. T. Soga, Y. Ohashi, Y. Ueno, H. Naraoka, M. Tomita, T. Nishioka, Quantitative metabolome analysis using capillary electrophoresis mass spectrometry. *J Proteome Res* **2**, 488-494 (2003).
46. H. Yamamoto, T. Fujimori, H. Sato, G. Ishikawa, K. Kami, Y. Ohashi, Statistical hypothesis testing of factor loading in principal component analysis and its application to metabolite set enrichment analysis. *BMC Bioinformatics* **15**, 51 (2014).

47. R. M. Duar, S. A. Frese, X. B. Lin, S. C. Fernando, T. E. Burkey, G. Tasseva, D. A. Peterson, J. Blom, C. Q. Wenzel, C. M. Szymanski, J. Walter, Experimental Evaluation of Host Adaptation of Lactobacillus reuteri to Different Vertebrate Species. *Appl Environ Microbiol* **83**, (2017).
48. K. Greisen, M. Loeffelholz, A. Purohit, D. Leong, PCR primers and probes for the 16S rRNA gene of most species of pathogenic bacteria, including bacteria found in cerebrospinal fluid. *J Clin Microbiol* **32**, 335-351 (1994).
49. D. Goldenberger, I. Perschil, M. Ritzler, M. Altwegg, A simple "universal" DNA extraction procedure using SDS and proteinase K is compatible with direct PCR amplification. *PCR Methods Appl* **4**, 368-370 (1995).
50. S. F. Altschul, W. Gish, W. Miller, E. W. Myers, D. J. Lipman, Basic local alignment search tool. *J Mol Biol* **215**, 403-410 (1990).
51. S. Kuraku, C. M. Zmasek, O. Nishimura, K. Katoh, aLeaves facilitates on-demand exploration of metazoan gene family trees on MAFFT sequence alignment server with enhanced interactivity. *Nucleic Acids Res* **41**, W22-28 (2013).
52. K. Katoh, J. Rozewicki, K. D. Yamada, MAFFT online service: multiple sequence alignment, interactive sequence choice and visualization. *Brief Bioinform* **20**, 1160-1166 (2019).
53. S. Kalyaanamoorthy, B. Q. Minh, T. K. F. Wong, A. von Haeseler, L. S. Jermiin, ModelFinder: fast model selection for accurate phylogenetic estimates. *Nat Methods* **14**, 587-589 (2017).
54. B. Q. Minh, H. A. Schmidt, O. Chernomor, D. Schrempf, M. D. Woodhams, A. von Haeseler, R. Lanfear, IQ-TREE 2: New Models and Efficient Methods for Phylogenetic Inference in the Genomic Era. *Mol Biol Evol* **37**, 1530-1534 (2020).
55. I. Letunic, P. Bork, Interactive Tree Of Life (iTOL) v5: an online tool for phylogenetic tree display and annotation. *Nucleic Acids Res* **49**, W293-W296 (2021).
56. D. Lane, "16s/23s rRNA sequencing" in *Nucleic Acid Techniques in Bacterial Systematics*, M. G. Erko Stackebrandt, Ed. (John Wiley & Sons, West Sussex, United Kingdom, 1991), pp. 115.
57. G. Muyzer, E. C. de Waal, A. G. Uitterlinden, Profiling of complex microbial populations by denaturing gradient gel electrophoresis analysis of polymerase chain reaction-amplified genes coding for 16S rRNA. *Appl Environ Microbiol* **59**, 695-700 (1993).
58. K. Matsuda, H. Tsuji, T. Asahara, K. Matsumoto, T. Takada, K. Nomoto, Establishment of an analytical system for the human fecal microbiota, based on reverse transcription-quantitative PCR targeting of multicopy rRNA molecules. *Appl Environ Microbiol* **75**, 1961-1969 (2009).
59. S. R. Herbel, B. Lauzat, M. von Nickisch-Rosenegk, M. Kuhn, J. Murugaiyan, L. H. Wieler, S. Guenther, Species-specific quantification of probiotic lactobacilli in yoghurt by quantitative real-time PCR. *J Appl Microbiol* **115**, 1402-1410 (2013).
60. A. M. Bolger, M. Lohse, B. Usadel, Trimmomatic: a flexible trimmer for Illumina sequence data. *Bioinformatics* **30**, 2114-2120 (2014).
61. G. Benson, Tandem repeats finder: a program to analyze DNA sequences. *Nucleic Acids Res* **27**, 573-580 (1999).
62. B. Langmead, S. L. Salzberg, Fast gapped-read alignment with Bowtie 2. *Nat Methods* **9**, 357-359 (2012).
63. D. E. Wood, J. Lu, B. Langmead, Improved metagenomic analysis with Kraken 2. *Genome Biol* **20**, 257 (2019).

64. J. Lu, F. P. Breitwieser, P. Thielen, S. L. Salzberg, Bracken: estimating species abundance in metagenomics data. *PeerJ Computer Science*, 3:e104 (2017).
65. F. Beghini, L. J. McIver, A. Blanco-Miguez, L. Dubois, F. Asnicar, S. Maharjan, A. Mailyan, P. Manghi, M. Scholz, A. M. Thomas, M. Valles-Colomer, G. Weingart, Y. Zhang, M. Zolfo, C. Huttenhower, E. A. Franzosa, N. Segata, Integrating taxonomic, functional, and strain-level profiling of diverse microbial communities with bioBakery 3. *Elife* **10**, (2021).
66. R. Caspi, T. Altman, K. Dreher, C. A. Fulcher, P. Subhraveti, I. M. Keseler, A. Kothari, M. Krummenacker, M. Latendresse, L. A. Mueller, Q. Ong, S. Paley, A. Pujar, A. G. Shearer, M. Travers, D. Weerasinghe, P. Zhang, P. D. Karp, The MetaCyc database of metabolic pathways and enzymes and the BioCyc collection of pathway/genome databases. *Nucleic Acids Res* **40**, D742-753 (2012).
67. C. Liu, Y. Cui, X. Li, M. Yao, microeco: an R package for data mining in microbial community ecology. *FEMS Microbiol Ecol* **97**, (2021).
68. J. Oksanen, G. L. Simpson, F. G. Blanchet, R. Kindt, P. Legendre, P. R. Minchin, R. O'Hara, P. Solymos, M. Stevens, E. Szoecs, Vegan: community ecology package, 2.6-2. *Vienna (Austria): R Foundation for Statistical Computing*, (2022).
69. A. Liaw, M. Wiener, Classification and regression by randomForest. *R news* **2**, 18-22 (2002).
70. R. Kolde, M. R. Kolde, Package 'pheatmap'. *R package* **1**, 790 (2015).
71. S. Nurk, D. Meleshko, A. Korobeynikov, P. A. Pevzner, metaSPAdes: a new versatile metagenomic assembler. *Genome Res* **27**, 824-834 (2017).
72. D. Li, R. Luo, C. M. Liu, C. M. Leung, H. F. Ting, K. Sadakane, H. Yamashita, T. W. Lam, MEGAHIT v1.0: A fast and scalable metagenome assembler driven by advanced methodologies and community practices. *Methods* **102**, 3-11 (2016).
73. V. Mallawaarachchi, Y. Lin, in *Research in Computational Molecular Biology. RECOMB 2022. Lecture Notes in Computer Science()*, I. Pe'er, Ed. (Springer, 2022), vol. 13278, pp. 70-85.
74. Y. W. Wu, B. A. Simmons, S. W. Singer, MaxBin 2.0: an automated binning algorithm to recover genomes from multiple metagenomic datasets. *Bioinformatics* **32**, 605-607 (2016).
75. D. D. Kang, F. Li, E. Kirton, A. Thomas, R. Egan, H. An, Z. Wang, MetaBAT 2: an adaptive binning algorithm for robust and efficient genome reconstruction from metagenome assemblies. *PeerJ* **7**, e7359 (2019).
76. C. M. K. Sieber, A. J. Probst, A. Sharrar, B. C. Thomas, M. Hess, S. G. Tringe, J. F. Banfield, Recovery of genomes from metagenomes via a dereplication, aggregation and scoring strategy. *Nat Microbiol* **3**, 836-843 (2018).
77. S. Pan, C. Zhu, X. M. Zhao, L. P. Coelho, A deep siamese neural network improves metagenome-assembled genomes in microbiome datasets across different environments. *Nat Commun* **13**, 2326 (2022).
78. J. N. Nissen, J. Johansen, R. L. Allesoe, C. K. Sonderby, J. J. A. Armenteros, C. H. Gronbech, L. J. Jensen, H. B. Nielsen, T. N. Petersen, O. Winther, S. Rasmussen, Improved metagenome binning and assembly using deep variational autoencoders. *Nat Biotechnol* **39**, 555-560 (2021).
79. J. Vollmers, S. Wiegand, F. Lenk, A. K. Kaster, How clear is our current view on microbial dark matter? (Re-)assessing public MAG & SAG datasets with MDMcleaner. *Nucleic Acids Res* **50**, e76 (2022).

80. A. Orakov, A. Fullam, L. P. Coelho, S. Khedkar, D. Szklarczyk, D. R. Mende, T. S. B. Schmidt, P. Bork, GUNC: detection of chimerism and contamination in prokaryotic genomes. *Genome Biol* **22**, 178 (2021).
81. D. H. Parks, M. Imelfort, C. T. Skennerton, P. Hugenholtz, G. W. Tyson, CheckM: assessing the quality of microbial genomes recovered from isolates, single cells, and metagenomes. *Genome Res* **25**, 1043-1055 (2015).
82. M. R. Olm, C. T. Brown, B. Brooks, J. F. Banfield, dRep: a tool for fast and accurate genomic comparisons that enables improved genome recovery from metagenomes through de-replication. *ISME J* **11**, 2864-2868 (2017).
83. P. A. Chaumeil, A. J. Mussig, P. Hugenholtz, D. H. Parks, GTDB-Tk: a toolkit to classify genomes with the Genome Taxonomy Database. *Bioinformatics*, (2019).
84. M. N. Price, P. S. Dehal, A. P. Arkin, FastTree 2--approximately maximum-likelihood trees for large alignments. *PLoS One* **5**, e9490 (2010).
85. H. Li, Minimap2: pairwise alignment for nucleotide sequences. *Bioinformatics* **34**, 3094-3100 (2018).
86. H. Mallick, A. Rahnavard, L. J. McIver, S. Ma, Y. Zhang, L. H. Nguyen, T. L. Tickle, G. Weingart, B. Ren, E. H. Schwager, S. Chatterjee, K. N. Thompson, J. E. Wilkinson, A. Subramanian, Y. Lu, L. Waldron, J. N. Paulson, E. A. Franzosa, H. C. Bravo, C. Huttenhower, Multivariable association discovery in population-scale meta-omics studies. *PLoS Comput Biol* **17**, e1009442 (2021).
87. D. D. Wang, L. H. Nguyen, Y. Li, Y. Yan, W. Ma, E. Rinott, K. L. Ivey, I. Shai, W. C. Willett, F. B. Hu, E. B. Rimm, M. J. Stampfer, A. T. Chan, C. Huttenhower, The gut microbiome modulates the protective association between a Mediterranean diet and cardiometabolic disease risk. *Nat Med* **27**, 333-343 (2021).
88. M. Strazar, G. S. Temba, H. Vlamakis, V. I. Kullaya, F. Lyamuya, B. T. Mmbaga, L. A. B. Joosten, A. van der Ven, M. G. Netea, Q. de Mast, R. J. Xavier, Gut microbiome-mediated metabolism effects on immunity in rural and urban African populations. *Nat Commun* **12**, 4845 (2021).

Fig. 1. Tameness is higher in selected mice compared to control. (A) Scheme of wild heterogenous stock generation; **(B)** Experimental timeline, **(C-E)** tameness test illustrative depiction, **(C)** active tameness test, **(D)** Passive tameness test, **(E)** stay-on-hand test, **(F-I)** active tameness test results, **(F)** heading, **(G)** contacting, **(H)** locomotion, **(I)** jumping, **(J-M)** passive tameness test results, **(J)** heading, **(K)** accepting, **(L)** locomotion, **(M)** jumping, **(N)** stay on hand test. N = 80 (20 in each group with 10 male and 10 female). (*$p<0.05$); **$p<0.01$; ***$p<0.001$). Bar graphs show means ± the SD with individual data points.

Fig. 2. Cladogram of 374 MAGs generated. (A) All 374 MAGs were placed in this cladogram generated by GTDB output. Different phylum was represented as different colours in the innermost circle. Second circle indicates size of each MAGs; Third circle indicates CheckM completeness and fourth circle indicates CheckM contamination. All novel MAGs are indicated as red star

Fig. 3. Gut microbiome diversity is similar in all groups. (A) Phylum level relative abundance in all groups, five most abundant phylum is shown; full dataset includes 11 phyla, 21 classes, 45 orders, 103 families, and 339 genera, **(B)** Ven diagram of 665 bacterial species present in WHS

mice gut, **(C)** Beta diversity based on Bray–Curtis dissimilarity, **(D)** Chao1 diversity, **(E)** Shannon diversity. **(F)** Hierarchical clustering using Pearson correlation distance between top 40 significantly different taxa (result of random forest analysis) with score of parameters of tameness test. Significant correlation is marked with "*" **(G)** Association analysis in MaAsLin2 between S2 group and bacterial abundance, **(H)** Association analysis in MaAsLin2 between S1 group and bacterial abundance, **(I-J)** MaAsLin2 generated graph of *Limosilactobacillus reuteri*, **(K-L)** MaAsLin2 generated graph of *Candidatus* Gallimonas intestinalis. N= 80 (20 in each group with 10 male and 10 female). (*p<0.05); ***p<0.001).

Fig. 4. Pyruvic acid is significantly high in selected mice. (A) Heatmap with hierarchical clustering using Pearson correlation distance of 70 metabolites identified, **(B-E)** Significantly higher metabolites before FDR correction, **(B)** Plasma pyruvic acid, **(C)** Plasma choline, **(D)** Plasma putrescine, **(E)** Plasma thymidine, **(F)** Plasma lactic acid, N = 12 (6 in each group). (*p<0.05); **p<0.01).

Fig. 5. *Limosilactobacillus reuteri* administration can increase tameness behaviour in mice. (A) Maximum likelihood tree of 16S rDNA region; different species of *Limosilactobacillus* genus was used for identification and *Lactobacillus helveticus* was used as outgroup. 1000 bootstrap was run and bootstrap value of more than 70% is shown with red ink. Bar graph represent pyruvate and lactate secretion in GAM media by different colonies of *L. reuteri* isolated in current study and *L. helveticus*, **(B)** scheme of bacteria administration to control mice through drinking water; **(C-G)** Different tameness test parameters after bacterial administration, **(C)** Active contacting, **(D)** Active heading, **(E)** Stay on hand test, **(F)** Passive heading, **(G)** passive accepting, **(H)** Serum pyruvate level after bacterial administration, **(I)** qRT-PCR quantification of *L. reuteri* present in faeces; (J) qRT-PCR quantification of *L. helveticus* present in faeces; N= 48 (12 in each group with 6 male and 6 female). N=48 for tameness test and q-PCR, N=40 for serum pyruvate concentration. (*p<0.05); **p<0.01; ***p<0.001). Bar graphs show means ± the SD with individual data points.

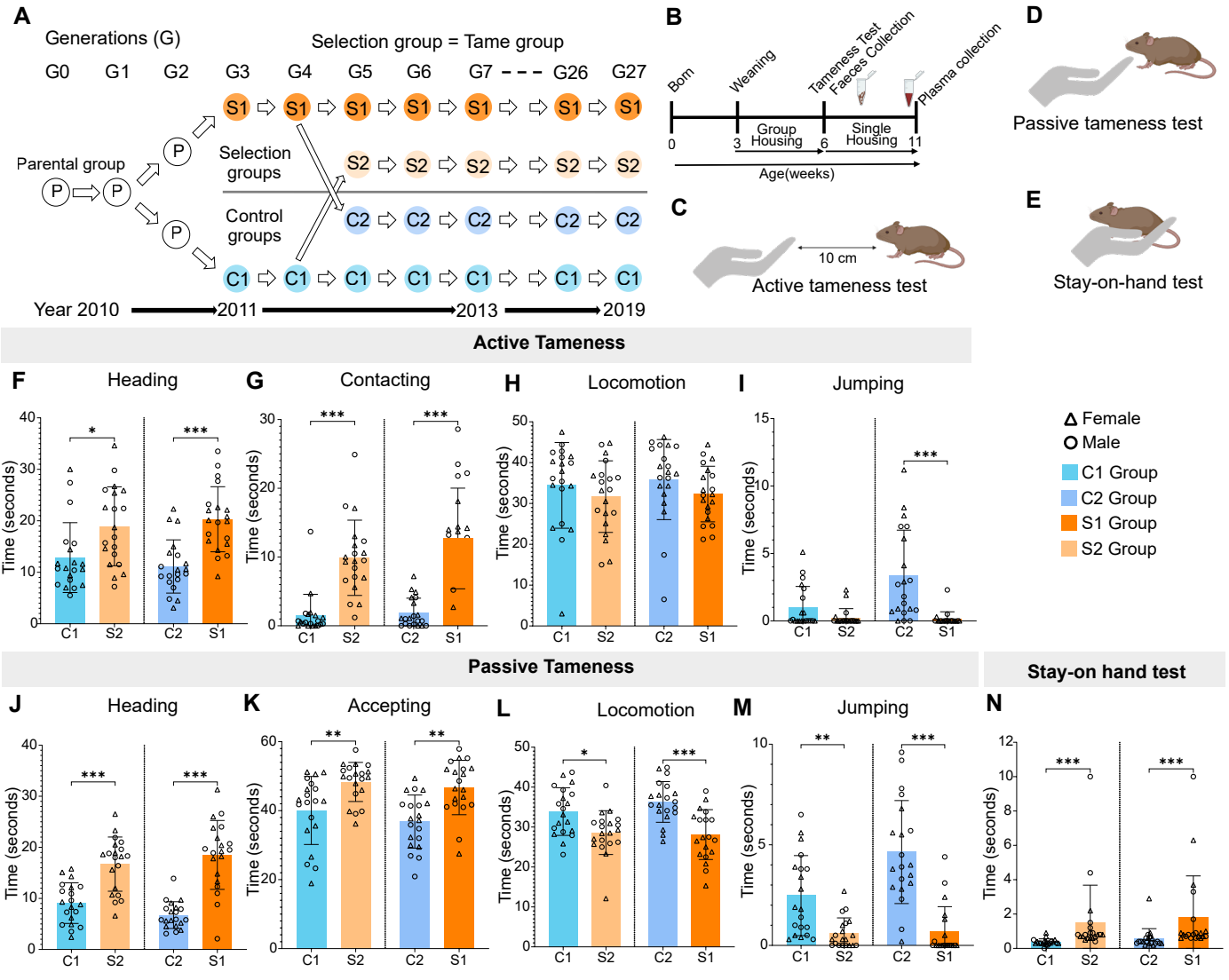
A
Generations (G)
Selection group = Tame group
G0 G1 G2 G3 G4 G5 G6 G7 - - - G26 G27
Parental group
P
Selection groups
Control groups
S1 S2 C2 C1
Year 2010 2011 2013 2019
B
Born
Weaning
Tameness Test
Faeces Collection
Plasma collection
Group Housing
Single Housing
0 3 6 11
Age(weeks)
C
10 cm
Active tameness test
D
Passive tameness test
E
Stay-on-hand test
Active Tameness
F Heading
G Contacting
H Locomotion
I Jumping
Time (seconds)
C1 S2 C2 S1
Female
Male
C1 Group
C2 Group
S1 Group
S2 Group
Passive Tameness
J Heading
K Accepting
L Locomotion
M Jumping
Stay-on hand test
N

Figure 1

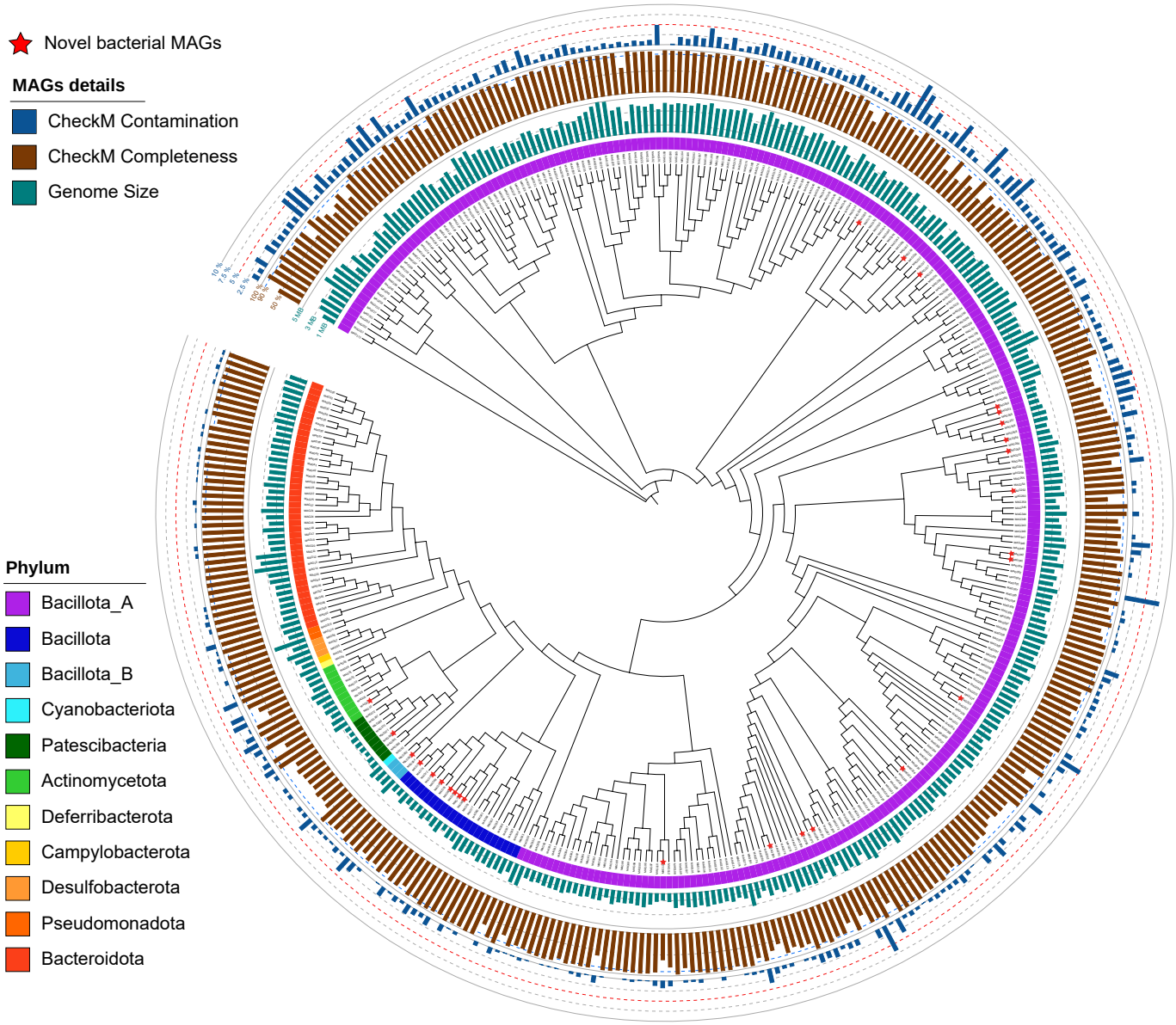
Novel bacterial MAGs
MAGs details
CheckM Contamination
CheckM Completeness
Genome Size
10 %
7.5 %
5 %
2.5 %
100 %
90 %
50 %
5 MB
3 MB
1 MB
Phylum
Bacillota_A
Bacillota
Bacillota_B
Cyanobacteriota
Patescibacteria
Actinomycetota
Deferribacterota
Campylobacterota
Desulfobacterota
Pseudomonadota
Bacteroidota

Figure 2

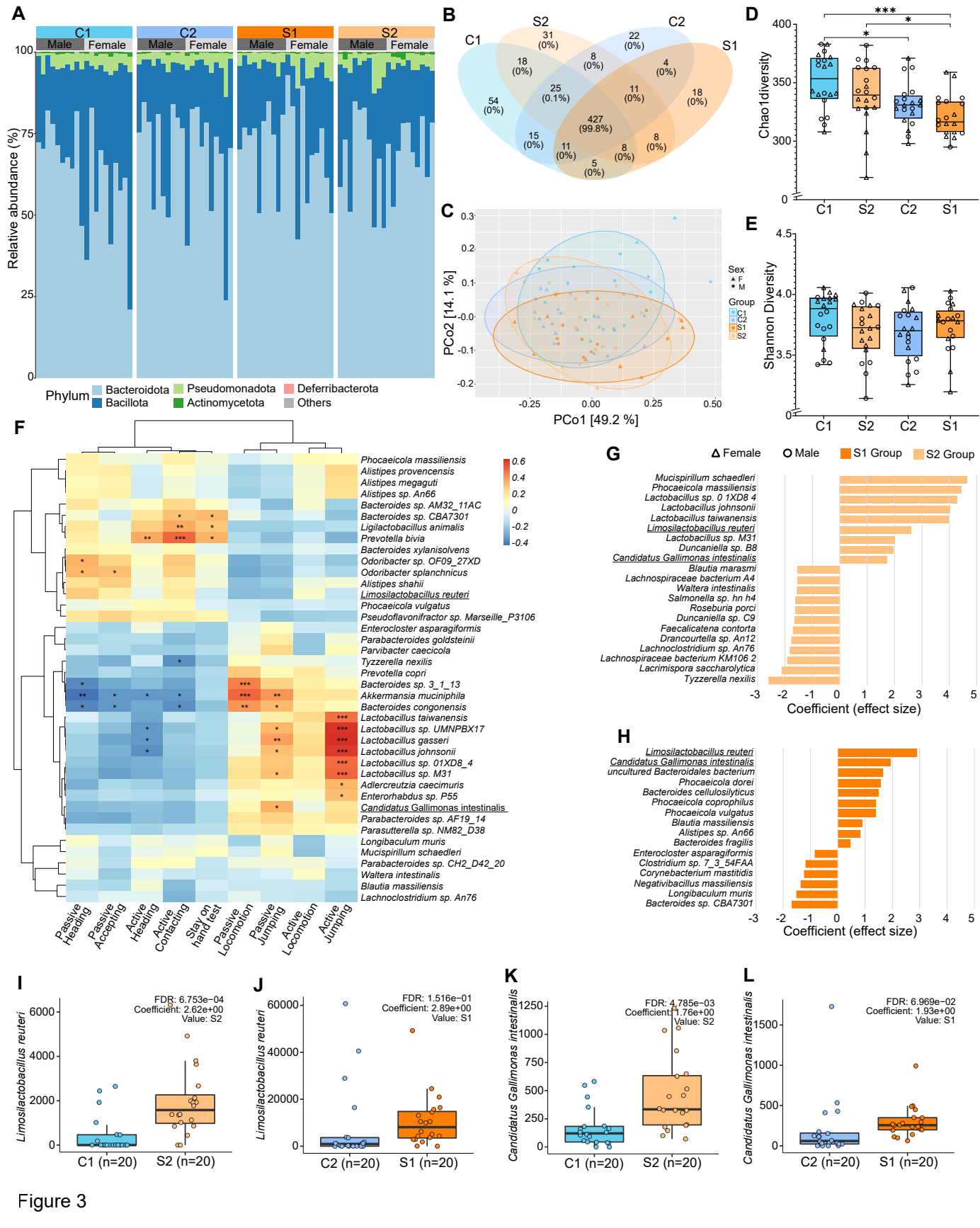
A
C1
C2
S1
S2
Male
Female
Relative abundance (%)
Phylum
Bacteroidota
Bacillota
Pseudomonadota
Actinomycetota
Deferribacterota
Others
B
C1
S2
C2
S1
54 (0%)
18 (0%)
31 (0%)
8 (0%)
22 (0%)
4 (0%)
25 (0.1%)
11 (0%)
18 (0%)
427 (99.8%)
15 (0%)
11 (0%)
8 (0%)
8 (0%)
5 (0%)
C
PCo2 [14.1 %]
PCo1 [49.2 %]
Sex
F
M
Group
C1
C2
S1
S2
D
Chao1diversity
E
Shannon Diversity
F
Passive Heading
Passive Accepting
Active Heading
Active Contacting
Stay on hand test
Passive Locomotion
Passive Jumping
Active Locomotion
Active Jumping
Phocaeicola massiliensis
Alistipes provencensis
Alistipes megaguti
Alistipes sp. An66
Bacteroides sp. AM32_11AC
Bacteroides sp. CBA7301
Ligilactobacillus animalis
Prevotella bivia
Bacteroides xylanisolvens
Odoribacter sp. OF09_27XD
Odoribacter splanchnicus
Alistipes shahii
Limosilactobacillus reuteri
Phocaeicola vulgatus
Pseudoflavonifractor sp. Marseille_P3106
Enterocloster asparagiformis
Parabacteroides goldsteinii
Parvibacter caecicola
Tyzzerella nexilis
Prevotella copri
Bacteroides sp. 3_1_13
Akkermansia muciniphila
Bacteroides congonensis
Lactobacillus taiwanensis
Lactobacillus sp. UMNPBX17
Lactobacillus gasseri
Lactobacillus johnsonii
Lactobacillus sp. 01XD8_4
Lactobacillus sp. M31
Adlercreutzia caecimuris
Enterorhabdus sp. P55
Candidatus Gallimonas intestinalis
Parabacteroides sp. AF19_14
Parasutterella sp. NM82_D38
Longibaculum muris
Mucispirillum schaedleri
Parabacteroides sp. CH2_D42_20
Waltera intestinalis
Blautia massiliensis
Lachnoclostridium sp. An76
G
Female
Male
S1 Group
S2 Group
Mucispirillum schaedleri
Phocaeicola massiliensis
Lactobacillus sp. 0 1XD8 4
Lactobacillus johnsonii
Lactobacillus taiwanensis
Limosilactobacillus reuteri
Lactobacillus sp. M31
Duncaniella sp. B8
Candidatus Gallimonas intestinalis
Blautia marasmi
Lachnospiraceae bacterium A4
Waltera intestinalis
Salmonella sp. hn h4
Roseburia porci
Duncaniella sp. C9
Faecalicatena contorta
Drancourtella sp. An12
Lachnoclostridium sp. An76
Lachnospiraceae bacterium KM106 2
Lacrimispora saccharolytica
Tyzzerella nexilis
Coefficient (effect size)
H
Limosilactobacillus reuteri
Candidatus Gallimonas intestinalis
uncultured Bacteroidales bacterium
Phocaeicola dorei
Bacteroides cellulosilyticus
Phocaeicola coprophilus
Phocaeicola vulgatus
Blautia massiliensis
Alistipes sp. An66
Bacteroides fragilis
Enterocloster asparagiformis
Clostridium sp. 7_3_54FAA
Corynebacterium mastitidis
Negativibacillus massiliensis
Longibaculum muris
Bacteroides sp. CBA7301
Coefficient (effect size)
I
FDR: 6.753e−04
Coefficient: 2.62e+00
Value: S2
Limosilactobacillus reuteri
C1 (n=20)
S2 (n=20)
J
FDR: 1.516e−01
Coefficient: 2.89e+00
Value: S1
Limosilactobacillus reuteri
C2 (n=20)
S1 (n=20)
K
FDR: 4.785e−03
Coefficient: 1.76e+00
Value: S2
Candidatus Gallimonas intestinalis
C1 (n=20)
S2 (n=20)
L
FDR: 6.969e−02
Coefficient: 1.93e+00
Value: S1
Candidatus Gallimonas intestinalis
C2 (n=20)
S1 (n=20)

Figure 3

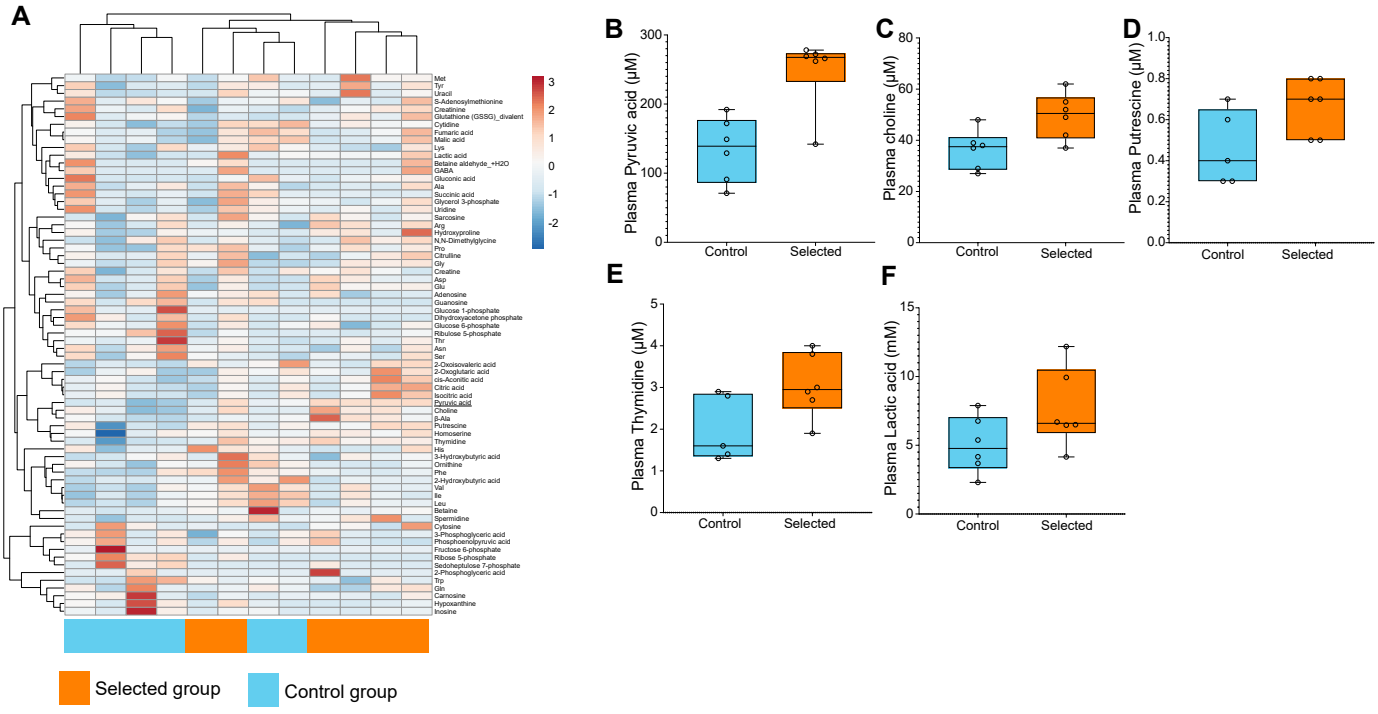
A
Met
Tyr
Uracil
S-Adenosylmethionine
Creatinine
Glutathione (GSSG)_divalent
Cytidine
Fumaric acid
Malic acid
Lys
Lactic acid
Betaine aldehyde_+H2O
GABA
Gluconic acid
Ala
Succinic acid
Glycerol 3-phosphate
Uridine
Sarcosine
Arg
Hydroxyproline
N,N-Dimethylglycine
Pro
Citrulline
Gly
Creatine
Asp
Glu
Adenosine
Guanosine
Glucose 1-phosphate
Dihydroxyacetone phosphate
Glucose 6-phosphate
Ribulose 5-phosphate
Thr
Asn
Ser
2-Oxoisovaleric acid
2-Oxoglutaric acid
cis-Aconitic acid
Citric acid
Isocitric acid
Pyruvic acid
Choline
β-Ala
Putrescine
Homoserine
Thymidine
His
3-Hydroxybutyric acid
Ornithine
Phe
2-Hydroxybutyric acid
Val
Ile
Leu
Betaine
Spermidine
Cytosine
3-Phosphoglyceric acid
Phosphoenolpyruvic acid
Fructose 6-phosphate
Ribose 5-phosphate
Sedoheptulose 7-phosphate
2-Phosphoglyceric acid
Trp
Gln
Carnosine
Hypoxanthine
Inosine
3
2
1
0
-1
-2
Selected group
Control group
B
Plasma Pyruvic acid (μM)
300
200
100
0
Control
Selected
C
Plasma choline (μM)
80
60
40
20
0
Control
Selected
D
Plasma Putrescine (μM)
1.0
0.8
0.6
0.4
0.2
0.0
Control
Selected
E
Plasma Thymidine (μM)
5
4
3
2
1
0
Control
Selected
F
Plasma Lactic acid (mM)
15
10
5
0
Control
Selected

Figure 4

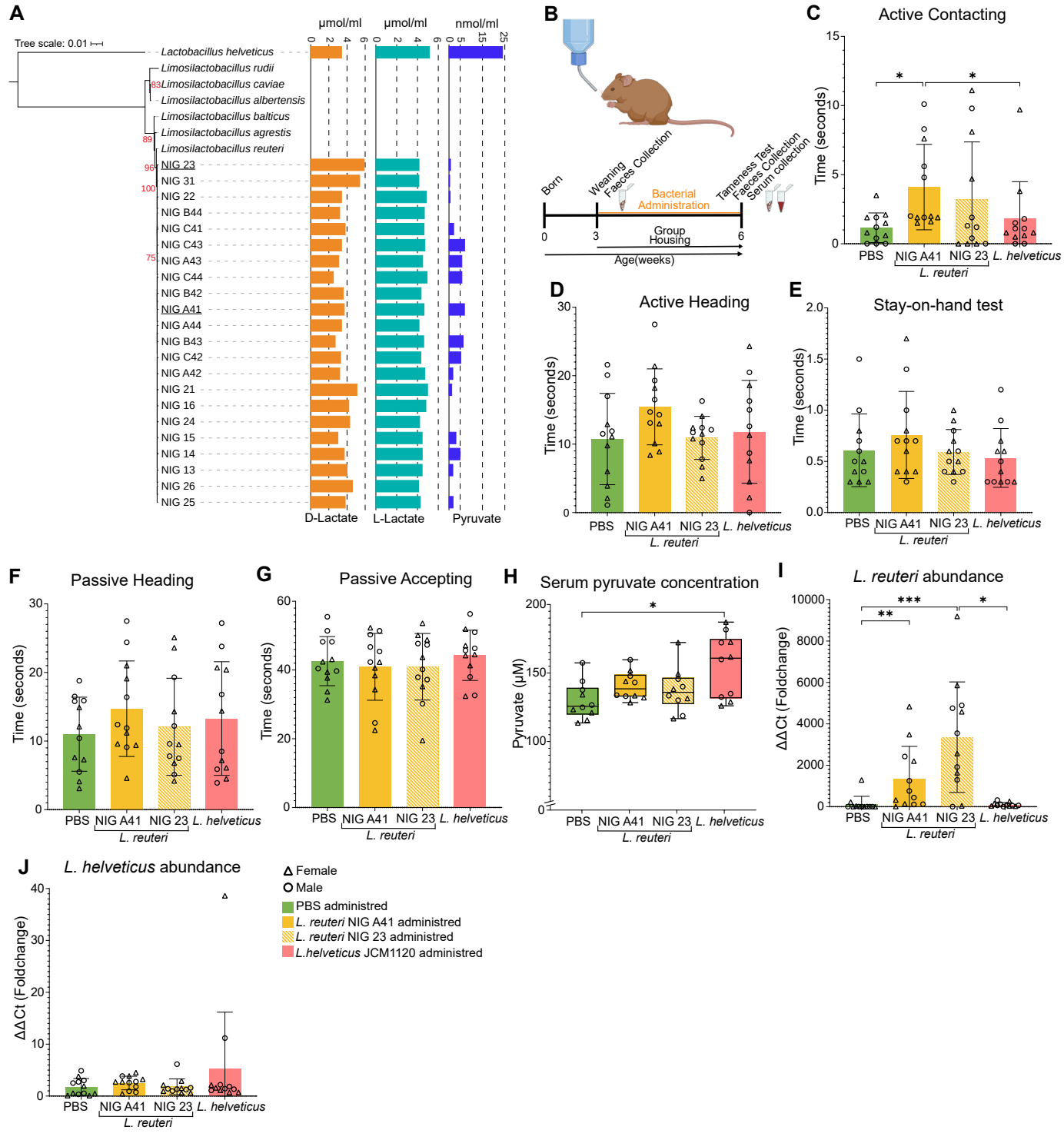
A
Tree scale: 0.01
Lactobacillus helveticus
Limosilactobacillus rudii
Limosilactobacillus caviae
Limosilactobacillus albertensis
Limosilactobacillus balticus
Limosilactobacillus agrestis
Limosilactobacillus reuteri
NIG 23
NIG 31
NIG 22
NIG B44
NIG C41
NIG C43
NIG A43
NIG C44
NIG B42
NIG A41
NIG A44
NIG B43
NIG C42
NIG A42
NIG 21
NIG 16
NIG 24
NIG 15
NIG 14
NIG 13
NIG 26
NIG 25
μmol/ml
μmol/ml
nmol/ml
D-Lactate
L-Lactate
Pyruvate
B
Born
Weaning
Faeces Collection
Bacterial Administration
Tameness Test
Faeces Collection
Serum collection
Group Housing
Age(weeks)
C
Active Contacting
Time (seconds)
D
Active Heading
Time (seconds)
E
Stay-on-hand test
Time (seconds)
F
Passive Heading
Time (seconds)
G
Passive Accepting
Time (seconds)
H
Serum pyruvate concentration
Pyruvate (μM)
I
L. reuteri abundance
ΔΔCt (Foldchange)
J
L. helveticus abundance
ΔΔCt (Foldchange)
PBS
NIG A41
NIG 23
L. helveticus
L. reuteri
Female
Male
PBS administred
L. reuteri NIG A41 administred
L. reuteri NIG 23 administred
L.helveticus JCM1120 administred

Figure 5